

International Journal of Vehicle Design

ISSN online: 1741-5314 - ISSN print: 0143-3369

https://www.inderscience.com/ijvd

Integrated real-time optimal energy management strategy for plug-in hybrid electric vehicles based on rule-based strategy and AECMS

Shaopeng Tian, Qingxing Zheng, Wenbin Wang, Qian Zhang

DOI: 10.1504/IJVD.2024.10061817

Article History:

Received: 29 April 2022 Last revised: 05 June 2023 Accepted: 12 June 2023 Published online: 23 January 2024

Integrated real-time optimal energy management strategy for plug-in hybrid electric vehicles based on rule-based strategy and AECMS

Shaopeng Tian, Qingxing Zheng*, Wenbin Wang and Qian Zhang

School of Automotive Engineering, Wuhan University of Technology,

Wuhan, 430070, China

Email: tianshp@whut.edu.cn Email: zqx@whut.edu.cn Email: 3083170284@qq.com Email: 372950295@qq.com *Corresponding author

Abstract: PHEVs have become one of the best market-oriented and industrialised technological routes in the automotive sector owing to fuel economy. To maximise the energy-saving potential of PHEVs, this study proposes an integrated real-time optimal strategy for a "P2+P4" PHEV. First, a rule-based mode-switching strategy was devised based on driving conditions. Second, an offline framework was established to optimise the equivalent factors (EFs) based on the firefly algorithm (FA). A novel EF adaptation law was then proposed based on the SOC feedback and duration of CD mode. Here, AECMS was employed to achieve optimal power allocation during CS mode. Finally, comparative simulations indicate that this PHEV can operate in CD mode for 55 km and 42.66 km under NEDC and WLTP, respectively. In CS mode, FA-AECMS has an approximate global optimal performance and a better charge-sustaining capability. Furthermore, the feasibility of the proposed strategy was validated using a drum experiment.

Keywords: plug-in hybrid electric vehicle; AECMS; adaptive equivalent consumption minimisation strategy; equivalent factors optimisation; firefly algorithm; a novel EF adaptation law.

Reference to this paper should be made as follows: Tian, S., Zheng, Q., Wang, W. and Zhang, Q. (2024) 'Integrated real-time optimal energy management strategy for plug-in hybrid electric vehicles based on rule-based strategy and AECMS', *Int. J. Vehicle Design*, Vol. 94, Nos. 1/2, pp.150–175.

Biographical notes: Shaopeng Tian received the BS from Wuhan University of Technology, Wuhan, China, in 1997 and the MSc in power machinery and engineering from Wuhan University of Technology, China, in 2000. In 2005, he received his PhD at Huazhong University of Science and Technology, Wuhan, China. His research interests include new energy vehicle powertrains, vehicle dynamics control, energy management of multi-energy vehicles, and intelligent electric platforms for new energy vehicles.

Qingxing Zheng received the BS in mechanical engineering from Wuhan University of Technology, China, in 2016. Since 2016, he has been studying PhD at the School of Automotive Engineering, Wuhan University of

Technology. His research interests include energy saving and new energy vehicles, design and development of new energy vehicle powertrains, and energy management of multi-energy vehicles.

Wenbin Wang received the BS from North University of China, China, in 2019 and the MSc in vehicle engineering from Wuhan University of Technology, China, in 2022. His research interest includes energy management for hybrid electric vehicles.

Qian Zhang received the BS from Zhengzhou University, China, in 2010 and the MSc in control theory and control engineering from Chongqing University of Posts and Telecommunications, China, in 2014. Now, he has been studying PhD at the School of Automotive Engineering, Wuhan University of Technology. His research interests include optimal control of hybrid electric vehicles and energy management of multi-energy vehicles.

1 Introduction

To address the energy crisis and greenhouse gas emissions, the Chinese government launched guidelines for peak and neutrality in carbon emissions (Hu et al., 2021; Wei et al., 2022; Zhao et al., 2022). With the overall goal of low-carbon development, decarbonisation has become a hot topic and focus in the automobile industry (Sabri et al., 2016; Martinez et al., 2016). In recent years, PHEVs have emerged as a lucrative alternative to solving the problem of dependence on fossil fuels and pollutant emissions (Zhou et al., 2019). PHEVs are equipped with at least two different energy storage systems for propulsion: an engine and an electric machine connected to a battery (Liu, 2013). A challenging problem that arises in this domain is improving the fuel economy by controlling the energy flow between the two power sources (Hu et al., 2016). Therefore, it is important to design advanced strategies for PHEVs.

1.1 Literature review

Based on previous research, two basic categories can be used to distinguish PHEV control strategies: rule-based and optimisation-based strategies (Li et al., 2016; Yang et al., 2017). The former has been widely used owing to its low computational cost and simple applications (Hao et al., 2016; Shen et al., 2018). The core issue is setting the rules of thumb based on the engine's optimal working area, engineering expertise, and optimisation result extraction (Fan et al., 2020). Sun (2021) developed a strategy based on an engine's optimal fuel consumption curve that exhibited excellent effectiveness and robustness in battery state of charge (SOC) control. Meng et al. (2017) devised an intelligent fuzzy strategy based on membership functions optimised using a genetic algorithm (GA) for PHEV, which functions well in fuel economy and battery SOC balance. Peng et al. (2017) developed a recalibration approach based on optimal control laws that were calculated using dynamic programming (DP). The experiments were conducted to highlight its superiority in terms of fuel economy.

Although the rule-based strategy is a simple method for splitting the power demand between multiple power sources in PHEVs, it cannot ensure optimum fuel efficiency under fixed thresholds. However, the optimisation-based strategy can maximise the energy-saving potential of PHEVs by optimising the torque allocation of the hybrid powertrain using different optimisation approaches. In general, it consists of global and instantaneous optimisation-based strategies. Among the global strategies, DP has been exploited by many researchers to obtain theoretical optimal solutions to energy management problems. Based on Bellman's principle, optimal solutions can be achieved by minimising cost functions with prior knowledge (Yang et al., 2014; Wang et al., 2021). Mojtaba et al. (2021) designed a predictive control strategy. A trained ANFIS model was devised to predict the reference SOC and power splitting was executed using DP. The simulations indicated that it is implementable and near-optimal in a real control environment. Liu et al. (2018) developed a DP-based strategy with a search range algorithm in which the velocity was predicted using a hybrid trip model. It can provide a practical solution for applying DP online in PHEV. In instantaneous optimisation-based strategies, model predictive control (MPC) and equivalent consumption minimisation strategy (ECMS) have been widely researched to resolve the energy management problem of the hybrid powertrain. MPC enables the planning of the energy allocation at a future time horizon with velocity prediction using the neural network (NN) and Markov chain (Xie et al., 2017; Liu et al., 2017). Fu et al. (2018) presented a two-layer MPC framework that planned the best SOC trajectory in a primary controller and achieved the optimal power split in the second controller, with an improvement in the fuel consumption and exhaust emissions. In the ECMS, the electricity consumption is converted into an equivalent fuel consumption using the equivalent factors (EFs). The torque split is executed further by minimising the instantaneous fuel consumption (Paganelli et al., 2002). Gao et al. (2017) presented a real-time strategy for PHEVs using ECMS to simultaneously reduce the total fuel consumption and maintain the battery SOC balance. Simulations and experiments validated its fuel economy and charge sustainability. Guo et al. (2019) also proposed a driving style-based ECMS by developing a hybrid PSO-GA to acquire the control laws between the driving style and EF. Compared with the ECMS, it can recognise driving styles and improve fuel economy under varied conditions.

For real-time optimisation, the ECMS has been successful in improving the fuel economy, where near-optimal results can be achieved under perfect EF settings (Sun et al., 2017). To reasonably tune the EFs, considerable research has been conducted to explore effective methods. A mathematical method was developed for calculating the lower and upper bounds of the EF based on theoretical energy flow analysis. Subsequently, an energy-saving opportunity-catching method was devised to obtain the optimal EF (Rezaei et al., 2018; Rezaei et al., 2019). Zeng et al. (2018) applied PSO to optimise the EF according to different driving patterns and initial battery SOCs. Then, the optimisation results were adopted as a two-dimensional map related to the battery SOC and driving distance. Consequently, the proposed simplified ECMS can decrease fuel consumption and shorten computational time. Xie et al. (2018) employed a shootingmethod-based PMP to determine the best EFs under multiple driving patterns, and the optimisation results were used to devise an ANN-ECMS. The proposed ANN-ECMS demonstrates satisfactory fuel economy and real-time performance. However, the aforementioned methods depend on prior knowledge and expert experience and cannot guarantee perfect results under actual conditions. Musardo et al. (2005) used an adaptive equivalent consumption minimisation strategy (AECMS) to address this issue, which allowed instantaneous adjustment of the EF under various driving conditions. Lei et al. (2020) leveraged a simplified DP to obtain the reference SOC and employed a fuzzy controller to adjust the EF based on the SOC deviation from the reference value. Besides, there has been significant research on the use of AECMS to adjust the EF based on the SOC deviation, such as using a feedback controller (Zhao et al., 2015) and a fuzzy sliding mode controller (Guan et al., 2019). Zhang et al. (2017) developed a multistep velocity prediction approach using V2V and V2I information and a CNN. A novel EF adaptation law was then proposed based on the predicted velocity and SOC feedback. The simulation indicated that it can achieve better fuel economy and SOC charge-sustaining improvements compared to the traditional AECMS. To incorporate traffic information into ECMS, Sun et al. (2022) established a road-type-based Markov velocity prediction model for SOC planning whereby the AECMS can adjust the EFs according to the reference SOC. Comparative simulations were then conducted to show the superiority of this strategy in reducing fuel consumption relative to the ECMS. Zhang et al. (2021) devised an optimisation framework to achieve adaptive energy management for an automated HEV. The flexible torque request was involved with the fuel economy objective to optimise the shift schedule and torque split based on ECMS. Consequently, simulation results demonstrate its high fuel economy and traffic efficiency.

1.2 Main contributions

As discussed above, the aforementioned ECMS-based strategies can adjust the EF through SOC feedback control based on the deviation from the reference SOC. However, SOC planning is executed based on the predicted knowledge of the driving conditions, or V2V and V2I information. The existing on-board controllers cannot satisfy the requirements of predictive AECMS in terms of the computational power and data storage capacity. Therefore, the control effect in mass-produced vehicles cannot be guaranteed. In addition, owing to the inconsistency in the sampling time between the hybrid control unit (HCU) and battery management system (BMS), a proper EF cannot be obtained in real-time using a simple SOC feedback-based EF adaptation law.

To address this problem, this study seeks to develop an integrated real-time optimal strategy for PHEVs. First, a rule-based strategy is employed to switch the vehicle's operation mode under complex driving conditions. Subsequently, the firefly algorithm (FA) is adopted to optimise the initial value of EFs based on a high-fidelity simulation model and target driving cycles, and the optimal results are further validated using a powertrain test bench. A novel EF adaptation law is then proposed by introducing a new element into the AECMS, the duration of the charge-depleting (CD) mode, which can be calculated by the HCU and reflects the initial SOC value before entering the charge-sustaining (CS) mode. Besides, the reference SOC calculation mechanism is simplified to an adjustable parameter determined by the driver. Hence, the EF can be reasonably adjusted based on the initial SOC and SOC deviation from the reference value. Finally, comparative numerical simulations are conducted to highlight its advantages, and the feasibility and real-time performance of the strategy in an actual vehicle environment are verified using a vehicle drum experiment.

1.3 Outline

The powertrain architecture and physical models of the PHEV are detailed in Section 2. The integrated real-time optimal strategy based on a rule-based vehicle operation

mode-switching strategy and an EF optimisation-based AECMS is given in Section 3. In Section 4, the pure electric range and fuel consumption are tested under NEDC and WLTP. And the comparative results are analysed to verify the merits of FA-AECMS in the CS stage. In Section 5, the drum experiment is conducted to validate the feasibility of the proposed method. Finally, the conclusions are presented in Section 6.

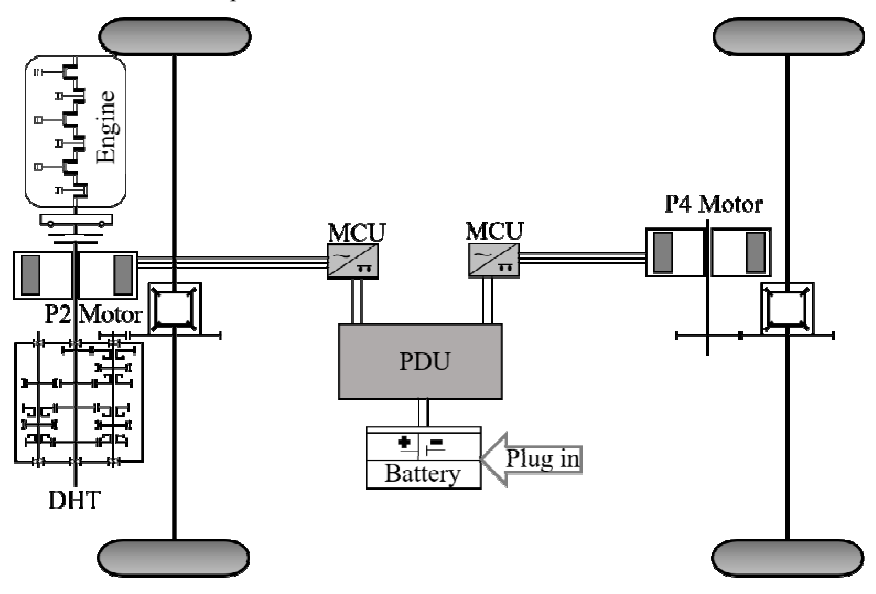
2 System description and vehicle modelling

A parallel hybrid electric powertrain with a P2+P4 configuration was studied (Wu et al., 2015) based on one of the most popular prototypes in the Chinese market, as shown in Figure 1. The engine and P2 motor were mounted on the front axle, and hybrid power coupling was achieved using an electromagnetic clutch. Additionally, the flywheel was attached to the input shaft of a six-gear dedicated hybrid transmission (DHT), which can improve the operating areas of the power components and realise speed reduction and torque increase. The P4 motor and a single-level main reducer were mounted on the rear shaft of the vehicle. Table 1 lists the key powertrain parameters, and the model descriptions are presented in the following subsections.

 Table 1
 Powertrain parameters

Items	Parameter(Unit)	Value	
Vehicle	m(kg)	1943	
	g(N/kg)	9.8	
	C_r	0.01	
	$\rho (\mathrm{kg/m}^3)$	1.2	
	C_d	0.379	
	$A_f(\mathrm{m}^2)$	2.659	
	δ	1.12	
	r(m)	0.342	
Transmission	i_g	[3.692 2.095 1.209 0.925 0.791 0.604]	
	i_f	[4.733 5.071]	
	i_r	7.7	
Engine	$P_{max}(kW)$	92	
	$T_{max}(Nm)$	234.7	
P2 Motor	$P_{max}(kW)$	105.4	
	$T_{max}(Nm)$	309	
P4 Motor	$P_{max}(kW)$	45	
	$T_{max}(Nm)$	170	
Battery	U(V)	350	
	Q(Ah)	37	

Figure 1 "P2+P4" PHEV powertrain



2.1 Vehicle longitudinal dynamics

Fuel economy, which is primarily reflected in the longitudinal motion of a vehicle, is crucial for developing a control strategy. Thus, only longitudinal dynamics are considered in this study. The wheel torque is calculated as follows:

$$T_{w} = (mgC_{r} + \frac{1}{2}\rho C_{d}A_{f}v^{2} + \delta m\frac{dv}{dt}) \cdot r, \qquad (1)$$

$$T_{w} = (T_{e}s_{clu} + T_{m,f}) \bullet i_{g} \bullet i_{f} \bullet \eta_{t} + T_{m,r} \bullet i_{r} \bullet \eta_{r} + T_{b},$$

$$\tag{2}$$

where T_e is the engine torque, $T_{m,f}$ and $T_{m,r}$ denote the P2 and P4 motor torques, respectively, T_b is the mechanical braking torque, s_{clu} represents the clutch state, η_t and η_r are the efficiency of the DHT and rear-axle main reducer, respectively, and v is the velocity.

2.2 Engine model

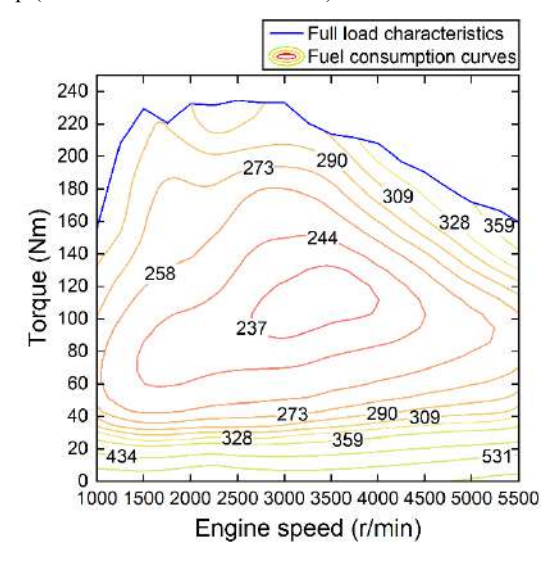
To reduce the computational effort, the internal combustion processes are ignored. Instead, a simplified engine model (Yang et al., 2018) is adopted to calculate the instantaneous fuel consumption (FC) based on the engine map shown in Figure 2.

$$\dot{m}_e(t) = \frac{T_e \omega_e b_e}{367.1 \rho_g g} \,, \tag{3}$$

$$b_e = f(\omega_e, T_e), \tag{4}$$

where b_e is the FC rate, ω_e is the engine speed, ρ_g is the gasoline density, and m_e is the instantaneous FC.

Figure 2 Engine map (see online version for colours)



The characteristics of the output torque should be modified to simulate the actual dynamic response process, which is expressed as:

$$T_e = \frac{1}{\tau_e s + 1} T_{e,com} \,, \tag{5}$$

where $T_{e,com}$ is the engine torque command from the energy management strategy and τ_e is the time constant.

2.3 Motor model

The P2 and P4 motors are PMSMs, which are simulated using the static method based on the motor efficiency data shown in Figure 3. The power consumption is calculated according to the motor torque, speed, and efficiency as follows:

$$\eta_{m} = f(\omega_{m}, T_{m}), \tag{6}$$

$$P_{m}(t) = \begin{cases} \frac{T_{m}(t)\omega_{m}(t)}{9550\eta_{m}} & T_{m} \ge 0\\ \frac{T_{m}(t)\omega_{m}(t)\eta_{m}}{9550} & T_{m} < 0 \end{cases}$$
(7)

where η_m represents the motor efficiency, f is the relationship function derived from the motor efficiency map, and ω_m , P_m , T_m represent the motor speed, power, and torque, respectively.

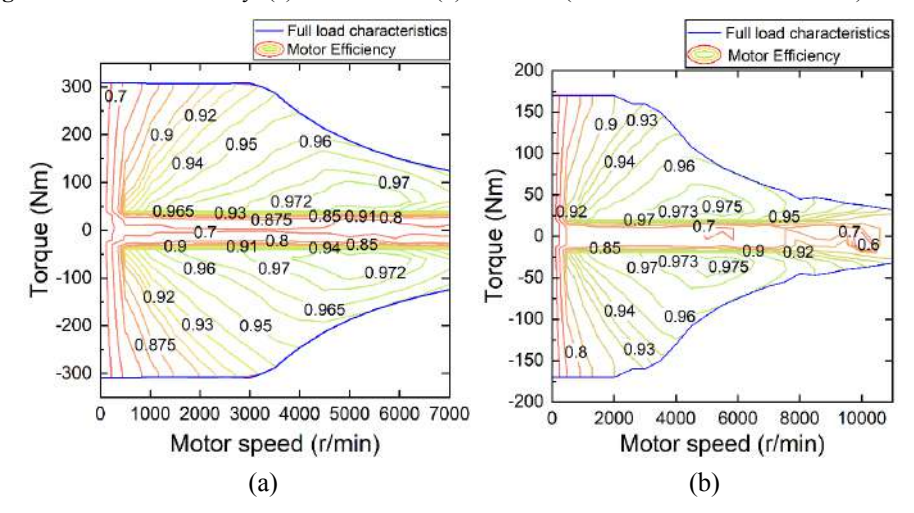


Figure 3 Motor efficiency: (a) P2 motor and (b) P4 motor (see online version for colours)

2.4 Battery model

It is challenging to construct an exact model that considers the electrochemical characteristics, temperature changes, and battery aging. In this study, the widely-adopted Rint model (Yang et al., 2020) is used for simplicity. The open-circuit voltage U_{oc} and inner resistance R_b are obtained using the function of SOC shown in Figure 4. The equations used are as follows:

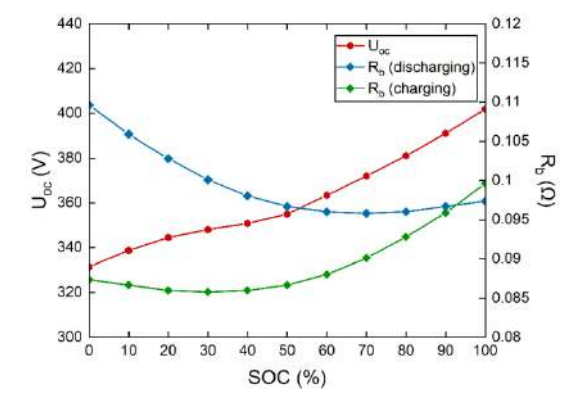
$$U_{oc} = f(SOC), R_b = f(SOC), \tag{8}$$

$$\dot{SOC} = -\frac{U_{oc} - \sqrt{U_{oc}^2 - 4R_b P_b}}{2R_b Q},$$
(9)

$$P_{bat} = P_b + I^2 R_b \,, \tag{10}$$

where Q denotes nominal capacity, P_b denotes the terminal power, P_{bat} denotes the input power, and I denotes the current.

Figure 4 Battery experimental data (see online version for colours)



2.5 DHT model

In this study, a six-gear DHT was used for the "P2+P4" PHEV. The shifting strategy and transmission ratio are closely related to the fuel economy and driving comfort (Wang et al., 2019). Thus, the transmission ratio was designed based on an offline optimisation, and a two-parameter shifting strategy was devised using the powertrain bench calibrations, as shown in Figure 5.

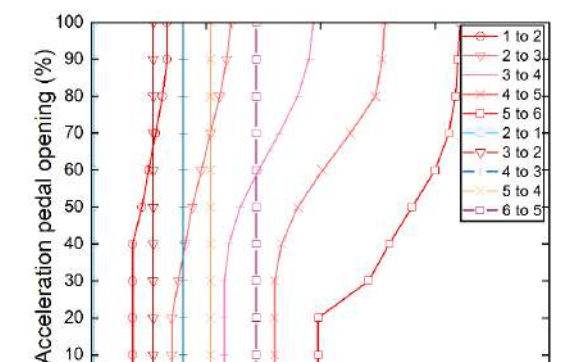


Figure 5 DHT shifting strategy (see online version for colours)

0

3 Integrated real-time optimal energy management strategy

PHEVs have high-capacity power batteries that allow vehicles to operate in pure electric mode for long periods and can be recharged at a low cost through external charging ports. In daily commuting or short-distance travel tasks, drivers are more willing to adopt the pure electric mode until the battery SOC drops to an allowable threshold. When the travel mileage exceeds the pure electric range of the PHEV, the vehicle is propelled by the engine and motor.

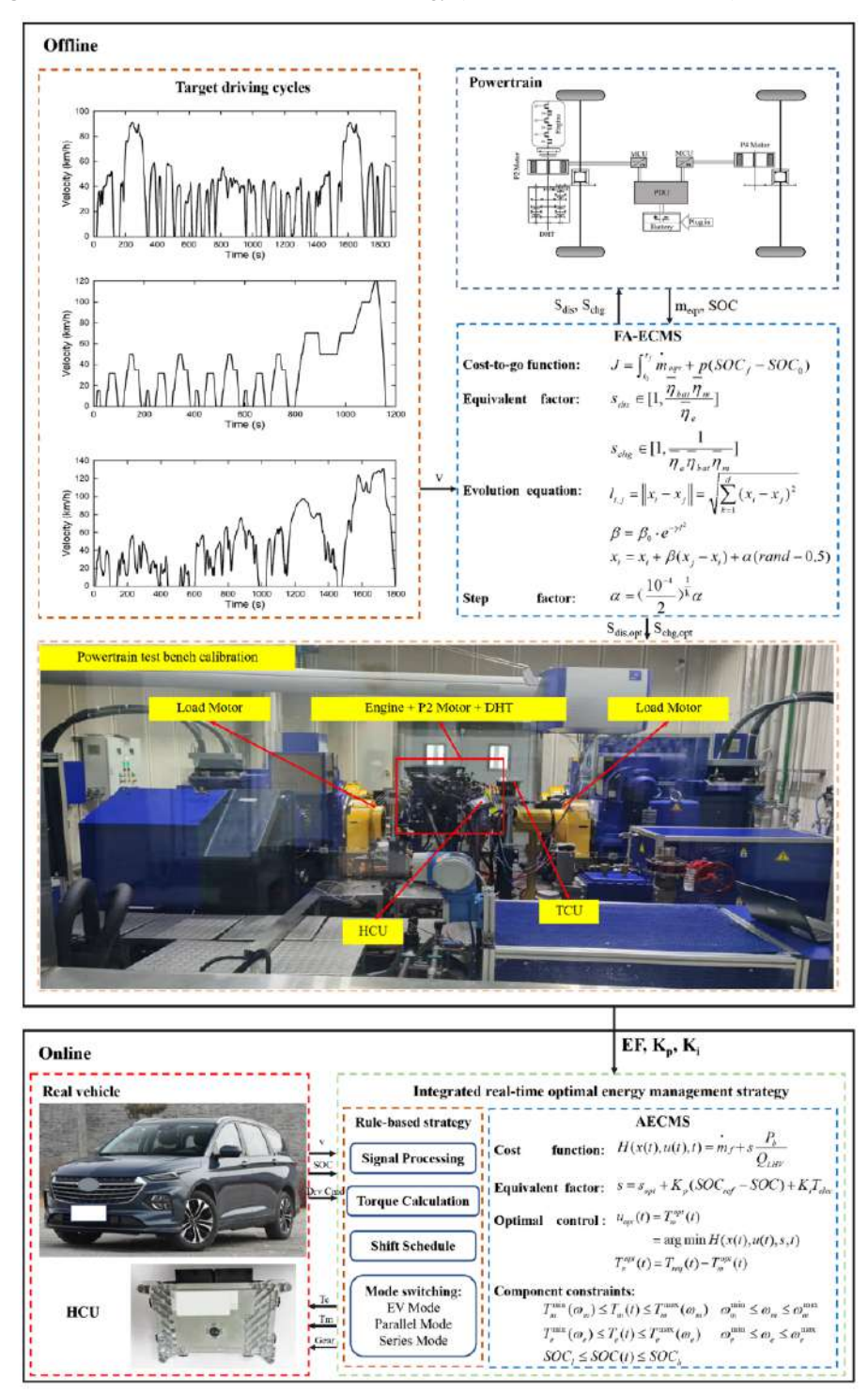
100

Velocity (km/h)

200

Considering the complicated and varied driving conditions, a hierarchical architecture was proposed based on the rule-based vehicle operation mode-switching strategy and EF optimisation-based AECMS for the PHEV, as shown in Figure 6. In the offline section, standard driving cycles were selected as the target driving cycles and a high-fidelity model was created and calibrated on a powertrain test bench. Subsequently, FA was adopted to optimise the initial value of EFs based on the high-fidelity simulation model and target driving cycles. Furthermore, the optimal EFs were validated and various control parameters such as K_p , K_l , and the mode-switching threshold were calibrated on a powertrain test bench. In the online section, a rule-based strategy was employed to switch the vehicle operation modes to adapt to complex driving environments and avoid inefficient engine operation. Subsequently, a novel AECMS was proposed to allocate the energy flow between the engine and battery by introducing a new element into the EF adaptation law to reflect the initial SOC value, that is, the duration of the CD mode before entering the CS mode.

Figure 6 Hierarchical architecture of the strategy (see online version for colours)



3.1 Rule-based vehicle operation mode switching strategy

In this study, the vehicle can be switched among three operation modes based on the varying power requirements and driver's command, in contrast to the CD-CS strategy in (Wirasingha et al., 2011). The three operation modes are series, CS, and CD, and each mode is represented by a specific number as listed in Table 2. In the CD mode, the P2 motor propels the vehicle, and the P4 motor only operates during the shifting process. Furthermore, the battery SOC gradually decreases until it reaches a designated threshold SOC_{ref} , which can be tuned between 30% and 80% by the driver and has a default value of 35%, and then maintains balance. The engine and P2 motor provide power in the CS mode. In the series mode, only the P4 motor propels the vehicle, and the engine and P2 motor work as a generator unit to charge the battery.

Series mode. When the SOC is <25%, the PHEV runs in the series mode. The series mode is designed as a limp-in mode wherein the P4 motor provides the entire propulsion torque, and the engine and P2 motor work as an electricity generation unit to charge the battery and satisfy the energy requirements of the P4 motor. However, because the P4 motor has a peak power of 45 kW and cannot satisfy large driving demands, the PHEV can only operate at a low velocity in the series mode.

CD mode. When the SOC is <35% or the EV mode button is activated, the PHEV operates in the CD mode. Here, only the P2 motor operates under most driving conditions, and the P4 motor propels the vehicle during the shifting process. Additionally, regenerative braking is permitted only when the SOC is <80% to avoid overcharging.

CS mode. When $25\% \le SOC < 35\%$ and the EV mode is not activated, the PHEV operates in the CS mode. Here, the engine and P2 motor operate jointly or separately to meet the driving torque, and the P4 motor supplies the torque during the shifting process. The torque split is based on the AECMS, as described in the following subsection. In the AECMS, the reference SOC is a variable parameter within the range of 30–80% and has a default value of 35%. The driver can adjust the reference SOC in the central control system according to the driving requirements. To ensure a satisfactory dynamic performance, the reference SOC should be higher than the mode-switching threshold of the series mode to minimise vehicle operation in series mode as much as possible.

Table 2	Vehicle operation mode
1.6	

Mode	Number	
CD mode	1	
CD2CS	2	
CS mode	3	
CS2CD	4	
X2S	5	
Series mode	6	
S2X	7	

In Table 2, CD2CS denotes a transition mode when the CD mode switches to the CS mode, CS2CD denotes a transition mode when the CS mode switches to the CD mode, X2S is a transition mode when another mode switches to the series mode, and S2X is a transition mode when the series mode switches to other modes.

3.2 Adaptive ECMS

The ECMS is an instantaneous optimisation approach that aims to minimise the FC at each instant by introducing a group of equivalent factors to convert the electricity consumption into an equivalent FC. Thus, the optimal torque split can be implemented. In this study, the FC is the overall target of the energy management problem, which is formulated as

$$F = \min J(u(t), x(t)). \tag{11}$$

Then, the control variable and the state variable are given as

$$\begin{cases} u(t) = T_m(t) \\ x(t) = SOC(t) \end{cases}$$
 (12)

Considering the actual mechanical and electrical characteristics of the powertrain, the control and state variables should satisfy the following limitations:

$$\begin{cases} T_{m}^{\min} \leq T_{m}(t) \leq T_{m}^{\max} \\ 0 \leq \omega_{m}(t) \leq \omega_{m}^{\max} \\ T_{e}^{\min} \leq T_{e}(t) \leq T_{e}^{\max} \\ 0 \leq \omega_{e}(t) \leq \omega_{e}^{\max} \\ SOC_{l} \leq SOC(t) \leq SOC_{h} \\ T_{dem} = T_{m}(t) + T_{e}(t) \\ SOC_{end} = SOC_{ini} \end{cases}$$

$$(13)$$

where J denotes the FC, T_m^{\min} , T_m^{\max} , T_e^{\min} and T_e^{\max} denote the maximum and minimum values of the P2 motor and engine torque, respectively, ω_m^{\max} and ω_e^{\max} denote the maximum value of the P2 motor and engine speed, respectively, T_{dem} denotes the demand torque, and SOC_{end} , SOC_{ini} denote the final and initial SOC, respectively.

By introducing the final SOC constraints into the objective function, equation (11) can be reformulated as follows:

$$J = \int_{t_0}^{t_f} \dot{m}_{eqv}(t)dt + f(SOC_{end} - SOC_{ini}),$$
 (14)

$$\left\{T_e^{opt}(t), T_m^{opt}(t)\right\} = \arg\min J, \qquad (15)$$

where m_{eqv} denotes the instantaneous equivalent FC, and f is a penalty related to the SOC_{end} .

Additionally, the expression of the equivalent FC is:

$$\dot{m}_{eqv}(t) = \dot{m}_{f}(t) + \dot{m}_{m-eqv}(t)
= \dot{m}_{f}(t) + s(t) \frac{P_{bat}(t)}{Q_{hv}},$$
(16)

$$s(t) = \left[s_{dis}(t), s_{chg}(t) \right], \tag{17}$$

where m_f is the engine FC, m_{m-eqv} is the equivalent FC of the electricity consumption, s represents the EF, and Q_{liv} denotes the low-heating value of gasoline.

To improve the adaptability of the ECMS, an AECMS was developed to dynamically change the EFs according to the SOC deviation. The core idea of the AECMS is that EFs weigh the battery energy based on the SOC deviation from its reference value. In other words, a negative deviation results in large EF values; thus, the battery energy becomes more expensive than the fuel. However, when the deviation is positive, the EFs have a small value, and as much battery energy as possible is used.

In general, a PI controller is adopted to calculate the EFs according to the SOC deviation from the SOC_{ref} at each moment. In this study, a novel element was introduced to the PI controller in addition to the SOC deviation to reflect the initial SOC value, that is, the duration of the CD mode before entering the CS mode T_{elec} . When the duration of the CD mode is short, T_{elec} has a small value, indicating that the fuel is more expensive than the electrical energy. Conversely, T_{elec} should be a large value to penalise the electricity consumption.

The adaptation law of equivalent factors is formulated as follows:

$$s_{dis}(t) = s_{dis,opt} + K_p(SOC_{ref} - SOC) + K_i T_{elec}$$

$$s_{chg}(t) = s_{chg,opt} + K_p(SOC_{ref} - SOC) + K_i T_{elec},$$
(18)

where $s_{dis,opt}$ and $s_{chg,opt}$ are the initial equivalent factors after offline optimisation using the FA, and K_p and K_i denote the control parameters of the PI controller.

3.3 Firefly algorithm

To exploit the optimality of the AECMS, a key challenge is the proper tuning of the initial EFs. EFs reflect the energy conversion efficiency of various power sources, which are affected by the characteristics of the powertrain and road types. Therefore, the problem of determining optimal EFs was formulated as a nonlinear global optimisation problem. The firefly algorithm is a novel method that mimics the behaviour of flashing fireflies (Yang, 2010). Our previous study proved that it has comparable global optimisation ability to the GA and PSO. Therefore, it was chosen for EF optimisation.

For the standard FA process, two essential factors have been proposed to mimic the behaviour of fireflies, luminance and attractiveness (Zheng et al., 2022). Fireflies with a higher fitness have a higher luminance and may be more attractive to their neighbours. However, their luminance decreases with the distance from other fireflies $l_{i,j}$, thereby affecting their attractiveness β . The steps of the FA are outlined below, as shown in Figure 7.

- 1 *Population initialisation*: A group of random fireflies is generated, and the positions of the fireflies are within the given range of EFs.
- 2 *Step factor calculation*: The step factor is varied nonlinearly from maximum to minimum in each iteration. The value is updated as follows:

$$\alpha = \alpha \frac{10^{-4}}{0.5}^{\frac{1}{k}},\tag{19}$$

where α denotes the step factor, and k represents the iteration number.

- 3 Luminance ranking: The position x of each firefly is used to represent the EFs, and its fitness value is selected as the luminance after the ECMS calculation. The fireflies are then sorted in order of luminance.
- 4 *Attractiveness calculation*: The luminance seen by nearby fireflies is used to determine how attractive each firefly is, which is defined as follows:

$$l_{i,j} = ||x_i - x_j|| = \sqrt{\sum_{k=1}^{d} (x_i - x_j)^2},$$

$$\beta = \beta_0 \cdot e^{-\gamma t^2},$$
(20)

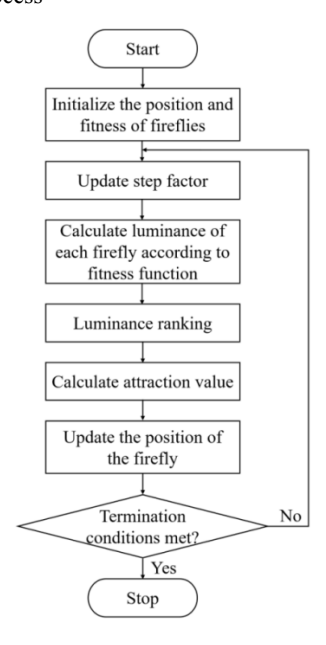
where β_0 is the initial value of β , γ is the light absorption coefficient.

5 *Update position*: The firefly movement process is determined as follows:

$$x_i = x_i + \beta(x_i - x_i) + \alpha(r - 0.5)$$
 (21)

6 Stopping rules: Steps (2)–(5) are repeated until the optimal EF is obtained.

Figure 7 FA optimisation process



3.4 Offline EF optimisation

The target driving cycles were selected according to GB/T19753-2021 in China. Therefore, the NEDC and WLTP were chosen. To obtain the optimal equivalent factors for the two driving cycles, the NEDC and WLTP were combined to form a longer driving cycle as the target driving cycle.

Subsequently, EF optimisation was performed. First, the FA was used to obtain the optimal equivalent factors based on the high-fidelity model. The candidates obtained after optimisation were then validated, and some control parameters were calibrated on a powertrain test bench. Finally, the above optimal solutions were written into a real HCU and used as control parameters to achieve optimal energy management.

4 Simulation results and analysis

In this section, the performance index of the PHEV was tested through the simulation. Based on the mode-switching strategy, the simulation was divided into CD and CS stages based on the SOC. The pure electric range and fuel consumption were then tested via simulations at different stages. The fixed-step Runge-Kutta method was selected as the solver. To ensure consistency with the real vehicle environment, the step size was set to 0.01 s.

4.1 Pure electric range simulation

In this section, the operating statuses of P2 and P4 motors in the CD stage were tested through the pure electric range simulation under NEDC and WLTP. The initial SOC was set to 100%.

As shown in Figure 8, the P2 motor can supply the power to track the desired velocity. The transmission can shift the gears from the second gear to the sixth gear according to the velocity and acceleration pedal opening. As the vehicle mileage increases, the battery SOC gradually decreases from 100%, and the hybrid state remains in the CD mode when the SOC is greater than 35%. However, it switches to the CS mode until the SOC drops to the switching threshold, which represents the end of the pure electric range simulation. The torque curves of the P2 and P4 motors are illustrated in the fourth rows of Figure 8(a) and (b). Under most operating conditions, the P2 motor propels the vehicle with the power it needs. However, when the transmission is shifting, the power of the front axle is lost, and the P4 motor acts as an auxiliary power source that provides the driving power to improve the vehicle's dynamic performance. The pure electric range and energy consumption are listed in Table 3. The battery capacity allows the PHEV to travel five NEDCs or approximately two WLTPs. The energy consumptions are 14.65 kWh/100 km and 15.36 kWh/100 km under the NEDC and WLTP, respectively. With the ending SOC of 35.32% and 35.01%, the pure electric ranges are 55 km and 42.66 km under the NEDC and WLTP, respectively, which verifies that this P2+P4 PHEV can operate in pure electric mode for long periods.

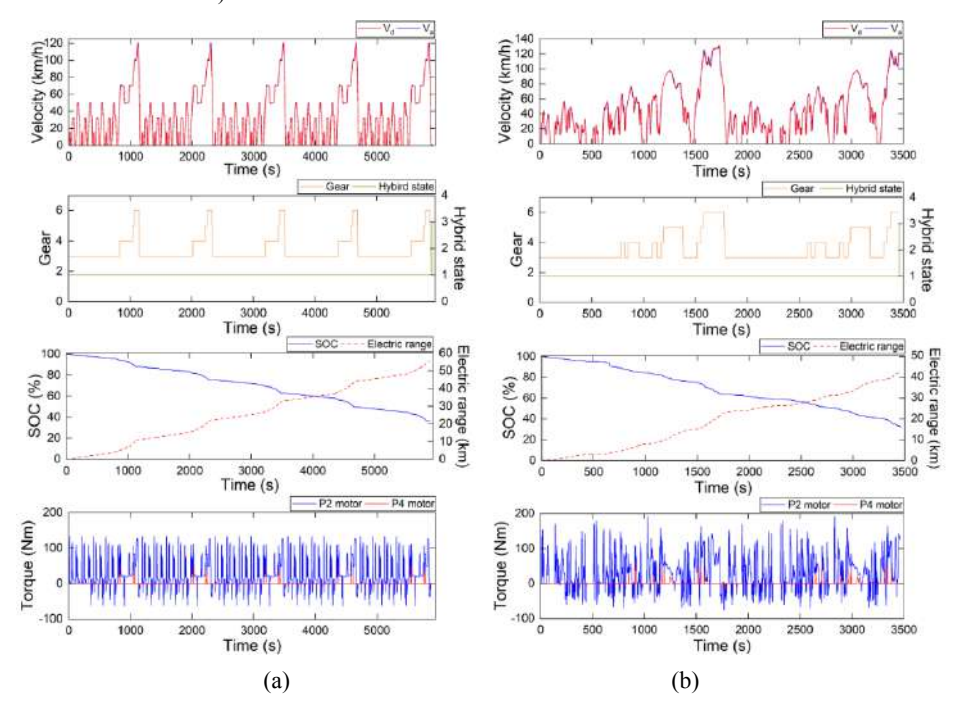
Driving cycle	Ending SOC (%)	Electric range(km)	Energy consumption (kWh/100 km)
NEDC	35.32	55	14.65
WTLP	35.01	42.66	15.36

Table 3 Energy consumption results in the CD stage

4.2 Fuel consumption simulation

This section consists of two parts. First, to prove the optimality of the FA-AECMS in the CS mode, the rule-based control strategy, traditional ECMS, and DP were used for comparison under two typical driving cycles. Then, the effectiveness of the EF adaptation law was evaluated in detail and compared with that of the traditional ECMS. The initial SOC was set to 35%.

Figure 8 Pure electric range simulation results: (a) NEDC and (b) WLTP (see online version for colours)

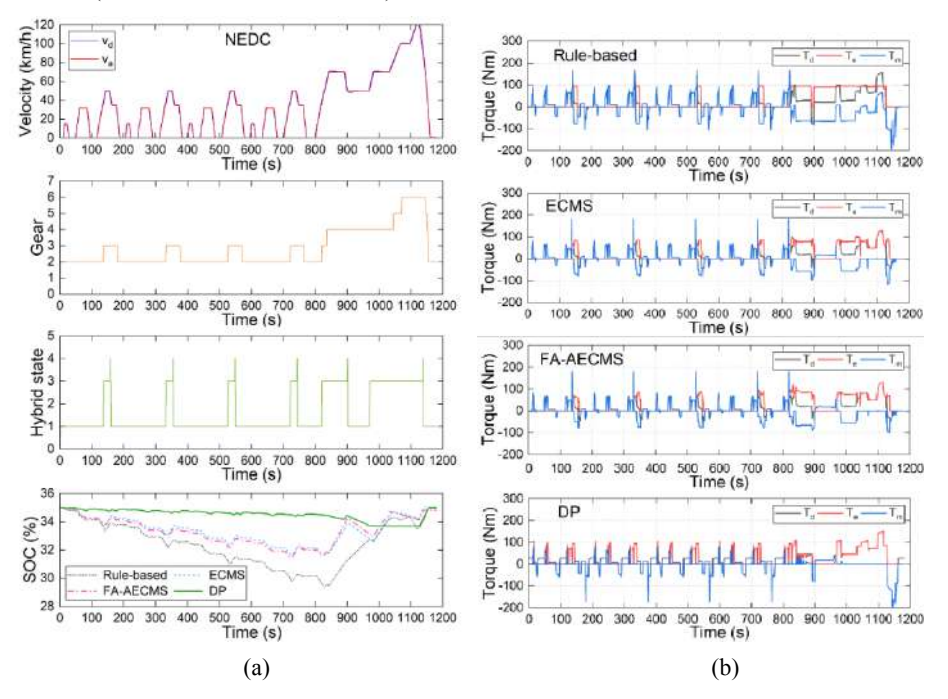


1 Comparative results of different control strategies

Figures 9 and 10 show the basic results, including the velocity, vehicle operation mode, gear shifting, battery SOC, and torque. As shown in Figure 9(a), the highest velocity error between the actual and desired velocities is less than 3 km/h, demonstrating that the devised energy management approach functions well. When the velocity is low, the P2 motor propels the vehicle, and the engine and P2 motor work together when the velocity

surpasses 45 km/h. Besides, the two-parameter shifting schedule functions well. In the fourth row of Figure 9(a), the ending SOCs for the four strategies are 34.97%, 35.01%. 34.81%, and 35%, respectively, demonstrating the charge-sustaining capabilities of the four strategies. Moreover, the SOC curve of the DP is more stable than those of the other three strategies, exhibiting global optimality in the energy management problems. The SOC tendencies of the ECMS and FA-AECMS are similar owing to the similar control logic. However, for the rule-based strategy, the SOC decreases sharply to 29%, causing the engine to begin propelling the vehicle and charging the battery. As shown in Figure 9(b), the engine and P2 motor can satisfy the hybrid powertrain's torque demand. Since the P4 motor only operates during the mode-switching process, it was neglected in the simulation. To avoid inefficient engine operation, the P2 motor drives the vehicle in low-torque-demand conditions, and the engine is used to provide the driving torque when the vehicle operates in high-torque-demand conditions to achieve better fuel economy. In the rule-based strategy, the engine torque is located in the optimal working area, and the engine torque trajectories of the ECMS and FA-AECMS are consistent. As for DP, the engine and motor solely or simultaneously provide the required torque according to optimal control law. The results in Figure 10 show a similar control effect in WLTP as in NEDC, although the velocity trajectory is more intense and the torque demand is larger than that in NEDC.

Figure 9 Comparison results for NEDC: (a) Velocity, gear, mode, SOC and (b) torque split (see online version for colours)



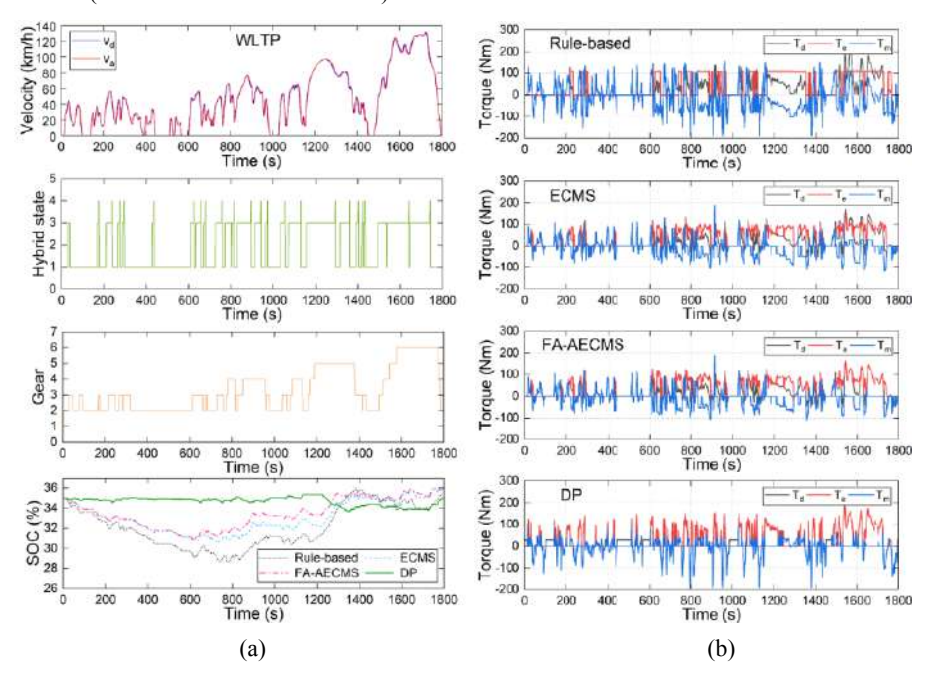


Figure 10 Comparison results for WLTP: (a) velocity, mode, gear, SOC and (b) torque split (see online version for colours)

Figure 11 illustrates the operation points of the engine and P2 motor. Although most engine operation points are located in the optimal working area, the high output power and long working time result in the worst fuel consumption results of the rule-based strategy. The distribution of engine operation points for the ECMS and FA-AECMS is similar in NEDC, while more operation points of the FA-AECMS are located in the optimal working area than those of the ECMS in WLTP. As for DP, its engine operation points are the best among the four strategies.

To further evaluate the optimality, the FC results are presented in Table 4. The FC of DP is regarded as the benchmark. When compared with the rule-based strategy, the FC improvements are 17.96% and 15.1% using the FA-AECMS in NEDC and WLTP, respectively. Because the advantage of the FA-AECMS is its adaptability to SOC changes, the improvement in fuel economy is relatively small compared with that of the ECMS. However, the FC of FA-AECMS is comparable to that of the DP, exhibiting an approximate global optimality. The computation times for FA-AECMS are listed in Table 5. The average computation time of ten simulations of NEDC and WLTP is 61.67 and 124.33 s, respectively, indicating a high real-time performance and real vehicle application potential.

Figure 11 Engine and motor operation points: (a) NEDC and (b) WLTP (see online version for colours)

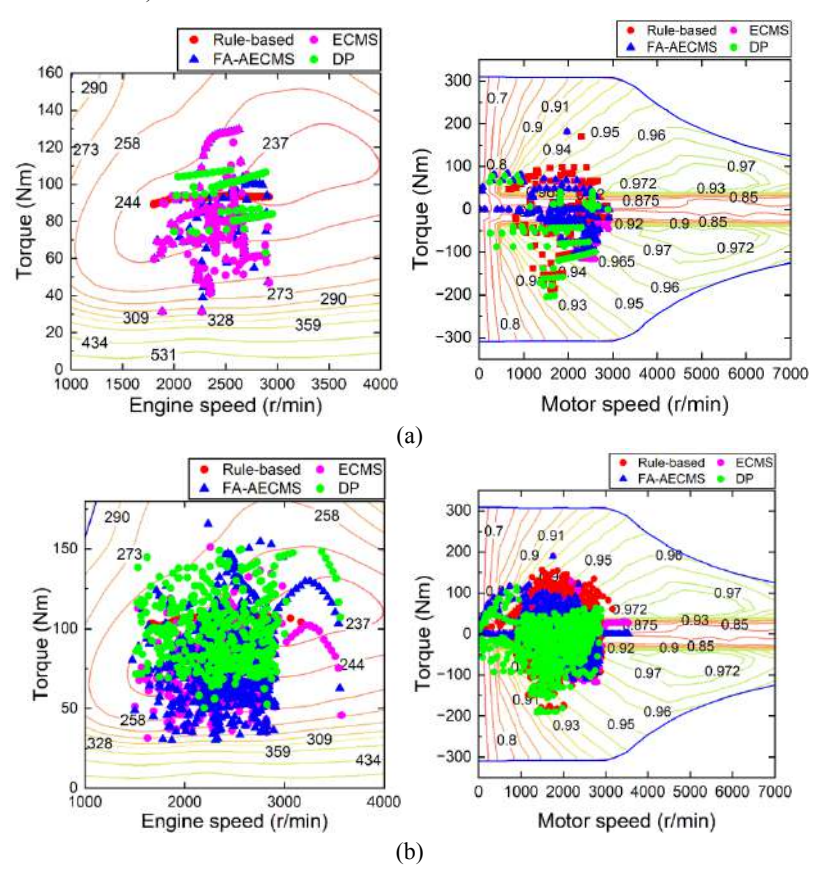


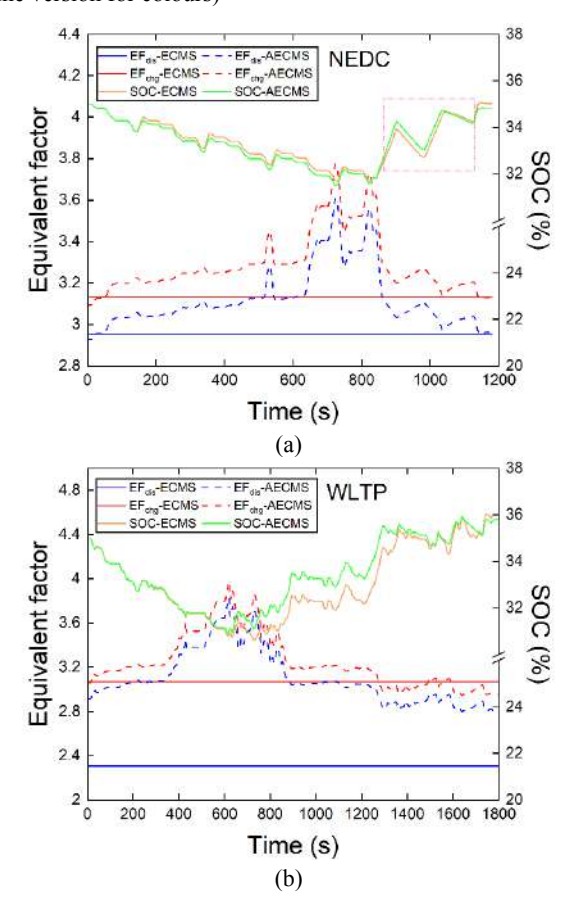
Table 4 Fuel consumption results in the CS stage

Driving cycle	Strategy	FC(L/100km)	Ending SOC(%)	Improvement(%)
NEDC	Rule-based	6.605	34.97	-20.79
	ECMS	5.648	35.01	-3.29
	FA-AECMS	5.623	34.81	-2.83
	DP	5.468	35	[-]
WLTP	Rule-based	7.409	35.33	-16.99
	ECMS	6.469	35.96	-2.14
	FA-AECMS	6.453	35.8	-1.89
	DP	6.333	34.99	[-]

 Table 5
 Computation time of the FA-AECMS

Driving cycle	Computation time (sing cycle Duration (s) (Avg value of 10 simula			
NEDC	1180	61.67		
WLTP	1800	124.33		

Figure 12 EF and SOC trajectories of ECMS and FA-AECMS: (a) NEDC and (b) WLTP (see online version for colours)



2 Superiority of the EF adaptation law

To further demonstrate the superiority of the EF adaptation law, the FA-AECMS was simulated and compared with the traditional ECMS. The comparative results, including the EF and SOC trajectories, are demonstrated in Figure 12. In the proposed strategy, when the SOC decreases, the EFs increase to penalise the electric energy consumption. In contrast, the EFs decrease when the SOC increases, making the motor the primary power source for propulsion. As for the ECMS, the EFs remain unchanged during the entire driving cycle. Furthermore, as shown in the zoomed-in area in Figure 12(a) and the area from 700 s to1400 s in Figure 12(b), the SOC trajectory of FA-AECMS is higher than that of ECMS. This is because the P2 motor consumes a large amount of electrical energy

in the first half of the simulation. Therefore, the EFs are updated to a large value to reduce electricity usage, thereby maintaining the battery SOC. However, the constant EFs cause a relatively sharp reduction of the battery SOC in the ECMS. These results show that the proposed EF adaptation law possesses excellent control performance and better charge-sustaining capability than the ECMS because the EFs can be adjusted according to the SOC deviation and duration of the CD mode.

5 Actual vehicle drum experiment

To assess the effectiveness and real-time performance, the HIL test and actual vehicle experiments are indispensable. Compared with the HIL test, the actual vehicle experiment is more authentic. Hence, an actual vehicle drum experiment was conducted to test the control performance and FC of the FA-AECMS. The four-wheel drum experiment bench consists of a circulating fan, wheel drum, exhaust emission detection device, and main console, as shown in Figure 13. During the experiment, the vehicle was fixed to the experiment bench. A circulating fan was then used to simulate a practical road wind environment, and the wheel drum was used as the loading device to simulate real road resistance based on the driving cycle. The exhaust emissions were then collected using a detection device and used to calculate the fuel consumption and pollutants. In this study, only the vehicle fuel consumption experiment was carried out according to GB/T19753-2021 in China. Standard NEDC and WLTP were then performed on the drum experiment bench, and the initial SOC was set to 35%. It is noteworthy that before the experiment, the vehicle was powered at a high voltage, and the shift lever was in forward gear.

Figure 13 Vehicle drum experiment: (a) drum experiment bench and (b) main console (see online version for colours)

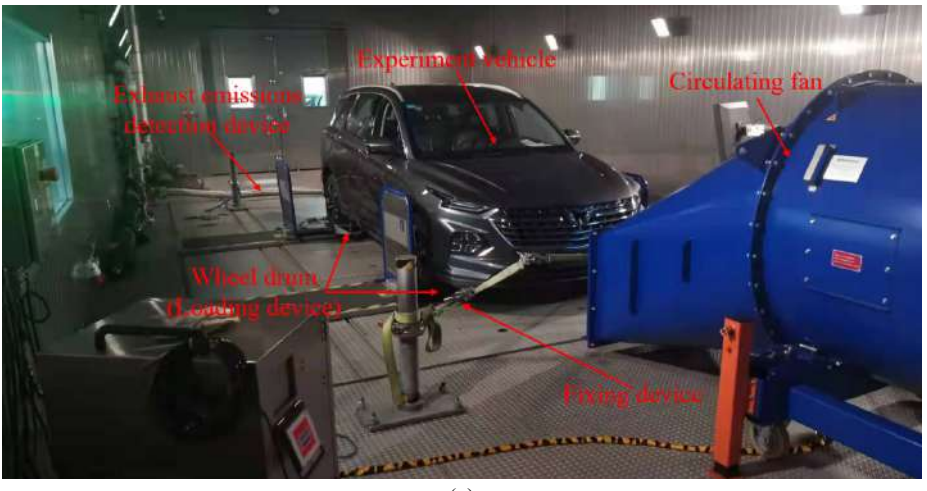


Figure 13 Vehicle drum experiment: (a) drum experiment bench and (b) main console (see online version for colours) (continued)

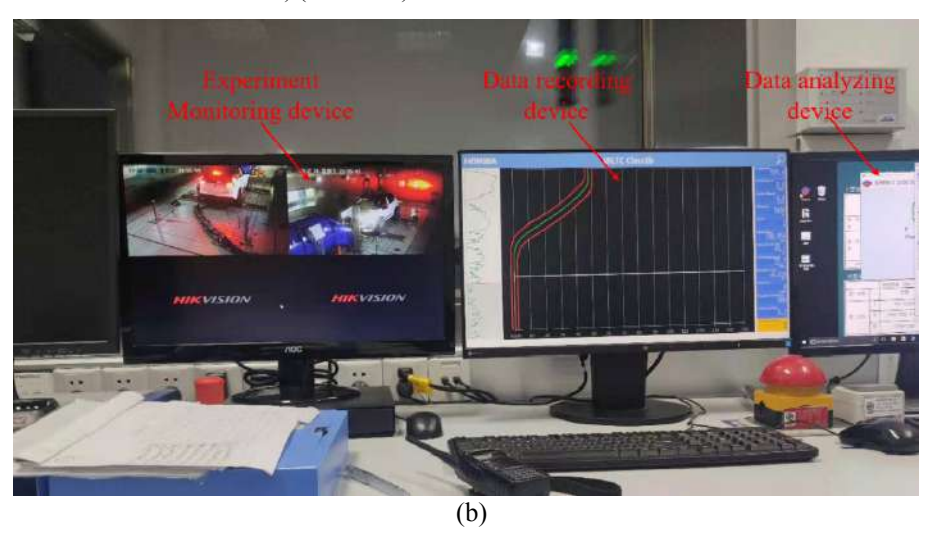


Figure 14 Comparative results of the simulation and experiment: (a) NEDC and (b) WLTP (see online version for colours)

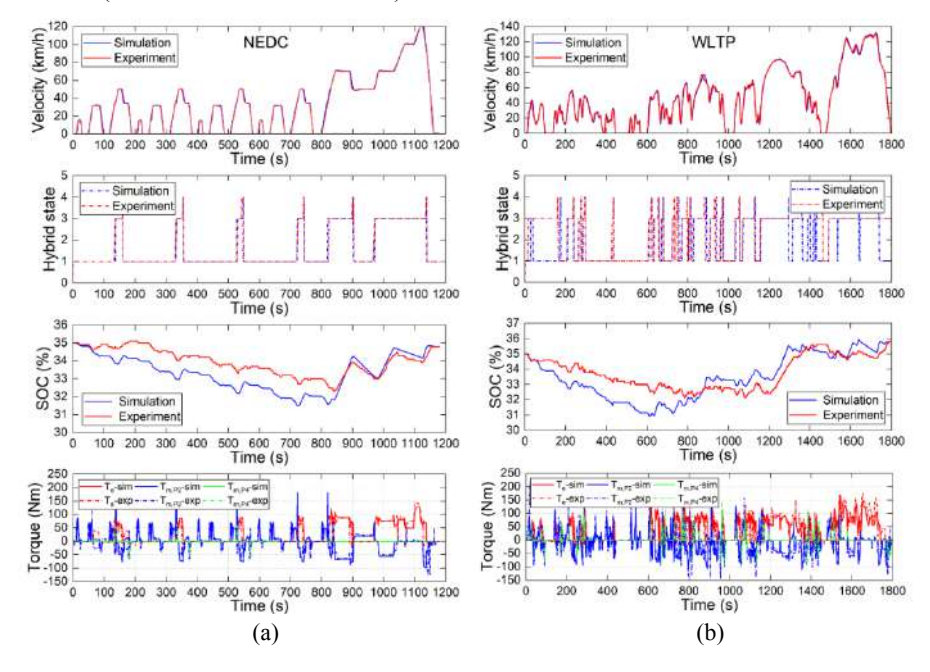


Figure 14 shows the results of the simulation and drum experiment. The velocity, vehicle operation mode, battery SOC, engine and motor torque are demonstrated. The error between the simulation and drum experiment is acceptable. As illustrated in Figure 14(a), the velocity curves of the simulation and drum experiment are consistent in the NEDC. The vehicle operation mode curves are also very similar, demonstrating that the rule-based mode-switching strategy functions properly both in the simulation and experiment.

Besides, the changing tendencies of the SOC, engine, P2 motor, and P4 motor torques are approximately the same. The comparative results for the WLTP are shown in Figure 14(b), and the same conclusion as that of the NEDC can be drawn. However, there are some differences in the results of the vehicle operation mode because the air conditioner is open and engine needs to be turned on. Thus, the vehicle operation mode is the CS mode in the experimental results from 0 s to 200 s, 1150 s to 1480 s, and 1500 s to 1800 s.

The FC results are listed in Table 6. The FC results of the drum experiment are slightly higher than those of the simulation. However, the final SOC of the drum test is basically the same as that of the simulation. Overall, the proposed strategy is proven to be practicable and exhibits excellent real-time performance in a real vehicle environment.

Item	Driving cycle	FC (L/100km)	Ending SOC (%)
Simulation	NEDC	5.623	34.806
	WLTP	6.453	35.796
Experiment	NEDC	5.787	34.8
	WLTP	6.702	35.8

 Table 6
 Comparative fuel consumption results

6 Conclusion

In this study, an integrated real-time optimal energy management strategy for PHEVs based on a rule-based vehicle operation mode switching strategy and an EF optimisation-based AECMS is proposed. The specific work can be summarised as follows:

- An integrated real-time optimal strategy that adopts a rule-based strategy to switch the vehicle operation mode to adapt to various driving conditions and a novel AECMS to optimise power allocation in the CS stage is proposed.
- 2 To obtain the optimal initial values of the EFs, two standard driving cycles, NEDC and WLTP, were combined to form the target driving cycle. Then, the FA was adopted to resolve the optimal EFs by minimising the fuel consumption. In addition, the optimal EFs were validated using a powertrain test bench. To improve the charge-sustaining capability of the AECMS, a novel EF adaptation law was proposed based on the SOC feedback and duration of the CD mode.
- To verify the optimality of the FA-AECMS in the CS stage, a comparison simulation involving the rule-based strategy, ECMS, and DP was conducted. The proposed strategy exhibits near-optimality during different driving cycles. Specifically, the fuel consumption using the FA-AECMS is reduced by 17.96% and 15.1% in the NEDC and WLTP, respectively, compared with that of the rule-based strategy. The FC improvement over the ECMS is relatively small, whereas the enhancement of the charge-sustaining capability is significant. The differences between the proposed strategy and DP are 2.83% and 1.89% in the NEDC and WLTP, respectively, indicating the near-optimality of the FA-AECMS. Furthermore, the drum experiment was conducted to verify its real-time performance. The results show that flexible

mode switching and optimal power splitting can be achieved in an actual vehicle environment.

In the future, with the accelerating advancement of cloud computing technology and intelligent transportation systems, the long-term prediction of the driving cycle will be possible. The influence of road type and driving behaviour characteristics on EF will be studied further, and a more intelligent energy management strategy should be developed for PHEVs with autonomous technology.

References

- Fan, L.K., Zhang, Y.T., Dou, H.S. and Zou, R.N. (2020) 'Design of an integrated energy management strategy for a plug-in hybrid electric bus', *Journal of Power Sources*, Vol. 448, pp.227391.
- Fu, J.T., Song, S.Z., Fu, Z.M. and Ma, J.W. (2018) 'Hierarchical model predictive control for parallel hybrid electrical vehicles', *Asian Journal of Control*, Vol. 20, No. 6, pp.2331–2342.
- Gao, A.Y., Deng, X.Z., Zhang, M.Z. and Fu, Z.M. (2017) 'Design and validation of real-time optimal control with ECMS to minimize energy consumption for parallel hybrid electric vehicles', *Mathematical Problems in Engineering*, Vol. 2017, No. 1, pp.1–13.
- Guan, J.C. and Chen, B.C. (2019) 'Adaptive power management strategy based on equivalent fuel consumption minimization strategy for a mild hybrid electric vehicle', *2019 IEEE Vehicle Power and Propulsion Conference*, Hanoi, Vietnam, pp.1–4.
- Guo, Q.Y., Zhao, Z.G., Shen, P.H., Zhan, X.W. and Li, J.W. (2019) 'Adaptive optimal control based on driving style recognition for plug-in hybrid electric vehicle', *Energy*, Vol. 186, pp.115824.
- Hao, J.X., Yu, Z.P., Zhao, Z.Z., Shen, P.H. and Zhan, X.W. (2016) 'Optimization of key parameters of energy management strategy for hybrid electric vehicle using DIRECT algorithm', *Energies*, Vol. 9, No. 12, p.997.
- Hu, J., Wu, J., Zhao, C. and Wang, P. (2021) 'Challenges for China to achieve carbon neutrality and carbon peak goals: Beijing case study', *PLoS One*, Vol. 16, No. 11, pp.e0258691.
- Hu, X., Moura, S.J., Murgovski, N., Egardt, B. and Cao, D. (2016) 'Integrated optimization of battery sizing, charging, and power management in plug-in hybrid electric vehicles', *IEEE Transactions on Control System Technology*, Vol. 24, No. 3, pp.1036–1043.
- Lei, Z.Z., Qin, D.T., Hou, L.L., Peng, J.Y., Liu, Y.G. and Chen, Z. (2020) 'An adaptive equivalent consumption minimization strategy for plug-in hybrid electric vehicles based on traffic information', *Energy*, Vol. 190, pp.116409.
- Li, L., You, S.X., Yang, C., Yan, B.J., Song, J. and Chen, Z. (2016) 'Driving-behavior-aware stochastic model predictive control for plug-in hybrid electric buses', *Applied Energy*, Vol. 162, pp.868–879.
- Liu, H., Li, X.M., Wang, W.D., Han, L.J. and Xiang, C.L. (2017) 'Markov velocity predictor and radial basis function neural network-based real-time energy management strategy for plug-in hybrid electric vehicles', *Energy*, Vol. 152, pp.427–444.
- Liu, J.C., Chen, Y.Z., Li, W., Shang, F. and Zhan, J.Y. (2018) 'Hybrid trip model based energy management of a PHEV with computation optimized dynamic programming', *IEEE Transactions on Vehicular Technology*, Vol. 67, No. 1, pp.338–353.
- Liu, W. (2013) Introduction to Hybrid Vehicle System Modeling and Control, Wiley, Cityspade Brandon, USA.
- Martinez, C.M., Hu, X., Cao, D., Velenis, E., Gao, B. and Wellers, M. (2016) 'Energy management in plug-in hybrid electric vehicles: recent progress and a connected vehicles perspective', *IEEE Transactions on Vehicular Technology*, Vol. 99, pp.4534–4549.

- Meng, D.W., Zhang, Y., Zhou, M.L. and Na, R.S. (2017) 'Intelligent fuzzy energy management research for a uniaxial parallel hybrid electric vehicle', *Computers and Electrical Engineering*, Vol. 58, pp.447–464.
- Mojtaba, H. and Zahra, R. (2021) 'An intelligent predictive controller for power and battery management in plug-in hybrid electric vehicles', *Journal of Energy Resources Technology*, Vol. 143, No. 11, pp.112105.
- Musardo, C., Rizzoni, G., Guezennec, Y. and Staccia, B. (2005) 'A-ECMS: an adaptive algorithm for hybrid electric vehicle energy management', *European Journal of Control*, Vol. 11, No. 4, pp.509–524.
- Paganelli, G. and Delprat, S. (2002) 'Equivalent consumption minimization strategy for parallel hybrid powertrains', *IEEE Vehicular Technology Conference*, Vol. 4, pp.2076–2081.
- Peng, J.K., He, H.W. and Xiong, R. (2017) 'Rule based energy management strategy for a series–parallel plug-in hybrid electric bus optimized by dynamic programming', *Applied Energy*, Vol. 185, pp.1633–1643.
- Rezaei, A., Burl, J.B. and Zhou, B. (2018) 'Estimation of the ECMS equivalent factor bounds for hybrid electric vehicles', *IEEE Transactions on Control System Technology*, Vol. 26, No. 6, pp.2198–2205.
- Rezaei, A., Burl, J.B., Zhou, B. and Rezaei, M. (2019) 'A new real-time optimal energy management strategy for parallel hybrid electric vehicles', *IEEE Transactions on Control System Technology*, Vol. 27, No. 2, pp.830–837.
- Sabri, M.F., Danapalasingam, K.A. and Rahmat, M.F. (2016) 'A review on hybrid electric vehicles architecture and energy management strategies', *Renewable and Sustainable Energy Reviews*, Vol. 53, No. 1, pp.1433–1442.
- Shen, P.H., Zhao, Z.G., Zhan, X.W., Li, J.W. and Guo, Q.Y. (2018) 'Optimal energy management strategy for a plug-in hybrid electric commercial vehicle based on velocity prediction', *Energy*, Vol. 155, No. 1, pp.838–852.
- Sun, C., Sun, F.C. and He, H.W. (2017) 'Investigating adaptive-ECMS with velocity forecast ability for electric vehicles', *Applied Energy*, Vol. 185, pp.1644–1653.
- Sun, J.X. (2021) 'Research on energy control strategy of PHEV', *IOP Conference Series: Earth and Environmental Science*, Vol. 714, p.042077.
- Sun, X.D., Cao, Y.F. and Jin, Z.J. (2022) 'An adaptive ECMS based on traffic information for plug-in hybrid electric buses', *IEEE Transactions on Industrial Electronics*, Vol. 99, pp.1–10.
- Wang, S.H., Huang, X.S., López, J.M., Xu, X.Y. and Dong, P. (2019) 'Fuzzy adaptive-equivalent consumption minimization strategy for a parallel hybrid electric vehicle', *IEEE Access*, Vol. 7, pp.133290–133303.
- Wang, W., Cai, Z.J. and Liu, S.F. (2021) 'Study on real-time control based on dynamic programming for plug-in hybrid electric vehicles', *SAE International Journal of Electrified Vehicles*, Vol. 10, No. 2, pp.167–176.
- Wei, Y., Chen, K., Kang, J., Chen, W., Wang, X. and Zhang, X. (2022) 'Policy and management of carbon peaking and carbon neutrality: a literature review', *Engineering*, Vol. 14, pp.52–63.
- Wirasingha, S.G. and Emadi, A. (2011) 'Classification and review of control strategies for plug-in hybrid electric vehicles', *IEEE Transactions on Vehicular Technology*, Vol. 60, No. 1, pp.111–122.
- Wu, G., Zhang, X. and Dong, Z.M. (2015) 'Powertrain architectures of electrified vehicles: review, classification and comparison', *Journal of the Franklin Institute*, Vol. 352, pp.425–448.
- Xie, S.B., Hu, X.S., Qi, S.W. and Lang, K. (2018) 'An artificial neural network-enhanced energy management strategy for plug-in hybrid electric vehicles', *Energy*, Vol. 163, pp.837–848.
- Xie, S.S., He, H.W. and Peng, J.K. (2017) 'An energy management strategy based on stochastic model predictive control for plug-in hybrid electric buses', *Applied Energy*, Vol. 196, pp.279–288.

- Yang, C., Du, S.Y., Li, L., You, S.X., Yan, Y.Y. and Zhao, Y. (2017) 'Adaptive real-time optimal energy management strategy based on equivalent factors optimization for plug-in hybrid electric vehicle', *Applied Energy*, Vol. 203, pp.883–896.
- Yang, C., You, S.X., Wang, W.D., Li, L. and Xiang, C.L. (2020) 'A stochastic predictive energy management strategy for plug-in hybrid electric vehicles based on fast rolling optimization', *IEEE Transactions on Industrial Electronics*, Vol. 67, No. 11, pp.9659–9670.
- Yang, S., Wang, W.S. and Zhang, F.Q. (2018) 'Driving-style-oriented adaptive equivalent consumption minimization strategies for HEVs', *IEEE Transactions on Vehicular Technology*, Vol. 67, No. 10, pp.9249–9261.
- Yang, S.C., Gu, Y. and Li, M. (2014) 'Offline optimization of parallel hybrid electric vehicle energy management strategy based on the dynamic programming', *Advanced Materials Research*, Vol. 1044, pp.941–946.
- Yang, X.S. (2010) 'Firefly algorithm, stochastic test functions and design optimization', International Journal of Bio-Inspired Computation, Vol. 2, No. 2, pp.78–84.
- Zeng, Y.P., Sheng, J. and Li, M. (2018) 'Adaptive real-time energy management strategy for plugin hybrid electric vehicle based on simplified-ECMS and a novel driving pattern recognition method', *Mathematical Problems in Engineering*, Vol. 2018, pp.1–12.
- Zhang, F.Q., Hu, X.S. and Langari, R. (2021) 'Adaptive energy management in automated hybrid electric vehicles with flexible torque request', *Energy*, Vol. 214, pp.118873.
- Zhang, F.Q., Xi, J.Q. and Langari, R. (2017) 'Real-time energy management strategy based on velocity forecasts using V2V and V2I communications', *IEEE Transactions on Intelligent Transportation Systems*, Vol. 18, No. 2, pp.416–430.
- Zhao, D.Z., Richard, S., Dong, G.Y. and Edward, W. (2015) 'Real-time energy management for diesel heavy duty hybrid electric vehicles', *IEEE Transactions on Control System Technology*, Vol. 23, No. 3, pp.829–841.
- Zhao, F., Liu, X., Zhang, H. and Liu, Z', 'Automobile industry under China's carbon peaking and carbon neutrality goals: challenges, opportunities, and coping strategies', *Journal of Advanced Transportation*, Vol. 2022, pp.1–13.
- Zheng, Q.X., Tian, S.P. and Wang, W.B. (2022) 'A comparative study of equivalent factor optimization based on heuristic algorithms for hybrid electric vehicles', *SAE International Journal of Sustainable Transportation, Energy, Environment, and Policy*, Vol. 3, No. 2, pp.187–201.
- Zhou, Y., Ravey, A. and Péra, M.C. (2019) 'A survey on driving prediction techniques for predictive energy management of plug-in hybrid electric vehicles', *Journal of Power Sources*, Vol. 412, No. 2, pp.480–495.